IEEE Access
Multidisciplinary | Rapid Review | Open Access Journal

Received December 29, 2020, accepted January 7, 2021, date of publication January 11, 2021, date of current version January 22, 2021.

Digital Object Identifier 10.1109/ACCESS.2021.3050704

EMG Biometric Systems Based on Different Wrist-Hand Movements

SUMIT A. RAURALE, (Member, IEEE), JOHN MCALLISTER, (Senior Member, IEEE), AND JESÚS MARTÍNEZ DEL RINCÓN, (Member, IEEE)

The Centre for Data Science and Scalable Computing (DSSC), Institute of Electronics, Communications and Information Technology (ECIT), Queen's University of Belfast, Belfast BT3 9DT, U.K.

Corresponding author: John McAllister (jp.mcallister@ieee.org)

This work was supported in a part by the Ph.D. project within School of Electronics, Electrical Engineering and Computer Science, Queen's University Belfast, U.K., from the Engineering and Physical Sciences Research Council (EPSRC), U.K., Studentship under Grant 2015–2019.

ABSTRACT Electromyogram (EMG) acquisition and analysis is growing in importance with human attempts to interact with and control equipment such as robots, prostheses or virtual environments. In some cases, only approved users should be permitted these capabilities. For these applications, securing EMG-based control is a major open question - to the best of the authors' knowledge, no prior art exists which can identify individuals from a wide range of wrist-hand gestures EMG readings within the wearable device. This paper addresses this problem. Techniques are presented which allow EMG to be used as a biometric, allowing users to verify themselves. An EMG-sensing armband attached to the lower forearm is used to anonymously authenticate users as a member of an approved group, or to identify themselves uniquely. For the development of extensive biometric system, three EMG datasets with similar EMG sensing in different sessions were exploited. For verification, accuracy of up to 93% is achieved, with 92% achieved for identification. The system is also shown to operate in real-time on an ARM Cortex A-53 embedded processor suitable for housing in an EMG wearable device, incurring latencies of 1.06 ms and 1.61 ms for verification and identification respectively. These metrics are comfortably sufficient for use in real-time, battery-powered EMG authentication devices.

INDEX TERMS Electromyogram (EMG), wrist-hand gestures, wearable device, biometric verification system, biometric identification system.

I. INTRODUCTION

Wearable technology has taken great strides in the past two decades due to significant advances in bio-physical signal processing and devices. In recent times, bio-electrical signals such as Electrocardiogram (ECG), Electromyogram (EMG) and Electroencephalogram (EEG) have increasingly been adopted for Human-Computer Interfacing (HCI) [1]. In particular, EMG devices can measure electrical currents generated in muscles during movement [2] and interpret these to control computers. This capability is crucial to enabling interaction with virtual reality video games via devices such as Optitrack gloves [3], physical exercise equipment like Datalite [4] or controlling robotic devices or 'bionic' prosthetic limbs such as Bebionic hand [5].

The EMG signal is generally acquired at the skin's surface and is a complex mix of electrical signals produced as a result of neuro-muscular activity, as well as the recording environment [2], [6]. Compared to other bio-electric signals, EMG signals vary widely subject to age, gesture style, muscle strength, motor unit paths and skin-fat layer [6]. Despite the complexity of the signals significant strides have been made in enabling their analysis; for instance, EMG acquired on the lower forearm have been shown to allow highly effective detection of specific wrist-hand gestures [7].

In many applications, though, detecting movements is not enough. This is particularly the case in applications where only skilled, trained or approved users should be allowed control of a piece of equipment. Whilst there has been much work on inferring limb movements based on EMG signals, unlike ECG and EEG [8], EMG-based authentication of users is a relatively poorly studied area. Despite the existence of numerous devices on the market, such as those outlined,

The associate editor coordinating the review of this manuscript and approving it for publication was Alba Amato.

where EMG is the only bio-physical signal measured, to the best of the authors' knowledge, there has been no work demonstrating the capacity to identify individuals based on their wrist-hand gestures within wearable EMG devices.

Two levels of authentication are desirable: the user can either be *verified* as one of an approved group of users, with or without *identifying* them uniquely [9], [10]. Three shortcomings are apparent in the current state-of-the-art:

- No current approach can, based only on wrist-hand EMG activity, authenticate whether an individual who remains anonymous is a member of an approved group of users [7], [8], [11], [12].
- No current approach can uniquely identify approved users from one-another via wrist-hand EMG activity alone [7], [8], [11].
- The lack of either of these two technologies precludes real-time EMG-based verification or identification for portable, battery-powered devices, as would be required for wearable HCI applications [13]–[16].

This paper makes the following contributions:

1) A novel authentication approach is described which uses multi-channel EMG sensed on the lower forearm to identify a user as a member of a pre-approved group, without requiring their unique identity, with up to 93% accuracy. One-time and continuous alternatives, which balance accuracy with complexity for different kinds of EMG equipment and HCI applications, are described.
2) An identification approach, based on the same EMG acquisition arrangement, is presented which can identify individual users via a wide range of wrist-hand gestures with accuracy in excess of 92%.
3) The proposed approaches are realised in real-time on a processor suitable for integration in portable, battery-operated EMG acquisition equipment required for EMG-based HCI. It is shown how either executes in less than 2 ms on an ARM Cortex A-53 processor.

Section II of this paper details types of biometric systems, before Section III and Section IV describe respectively the verification and identification approaches. Section V detailed their real-time implementations.

II. LITERATURE REVIEW

A. BIOMETRIC SYSTEMS

A biometric system is a pattern recognition system that distinguishes individuals or groups from one another by extracting information from biophysical signals [17]. Biometric systems have been demonstrated using fingerprint [13], face [14], voice [15], iris recognition [16], ECG [18]–[20] and/or EMG analysis [21]–[24]. Each offers a different balance of vulnerability, ease of use, obtrusiveness, and complexity.

Biometric systems can operate in two modes:

- *Verification*: a user is identified as belonging to a pre-determined approved group. Information extracted from input signals are compared with training data and when a match is identified, the user is permitted to control the equipment, otherwise they are denied [17]. Use-cases include specialised medical or other equipment which should only be controlled by trained, skilled users.
- *Identification*: the system recognises the user uniquely. It compares their biometric against a set of approved users. The user's identity is verified, or access is denied [17]. Use-cases include personalised devices, which should be under the control of only the user.

For verification, a variety of approaches have been used. Fingerprint [25], face [26] and iris recognition have all required user scanning with complex video processing [16]. These, however are not really bio-signals as such. Hammad *et al*. [19], [20] present an authentication approach using ECG which employs a Convolutional Neural Network (CNN) to provide authentication accuracy exceeding 99%. The fusion of multiple signal sources has also been used to increase biometric verification performance. For instance, [27] proposes two-factor verification using a person's fingerprint and [28] a system which fuses EEG and ECG to identify subjects with 97.90% accuracy. Some studies have tried using EMG analysis as part of such a fused approach. In [21], an individual is verified via EMG analysis of the heartbeat. In [29] the concept of biometric verification using multi-channel EMG signals corresponding to hand gestures was proposed, but not reported but no results have been presented. In [30] is presented an approach which verifies a person using keystroke dynamics while typing a password in addition to associated EMG signalling.

For identification, face, fingerprint, hand gestures and voice are commonly used [17]. Within bio-signals, ECG analysis has been commonly used [31], [32], with few studies on EMG analysis for person identification [22]–[24]. The work in Chan *et al*. [31] uses percent residual difference, correlation coefficient and wavelet distance to characterise single-lead ECG signals. Israel *et al.* [32] presents a multi-modal fusion of ECG and facial or palm recognition for user identification. Krishnamohan *et al*. [23] introduced the use of EMG signals from upwards motion of wrist for person identification using vector quantisation (VQ) and Gaussian mixture model (GMM) with 73.33% accuracy. Further, Kim *et al*. [22] presented a person identification technique based on EMG activity from various elbow-hand-finger movement using time domain features with Principal Component Analysis (PCA) and Linear Discriminant Analysis (LDA) followed by Euclidean Distance (ED), Support Vector Machine (SVM), and K-Nearest Neighbour (KNN) resulting 86.66% accuracy. More recently, Chantaf *et al*. [24] used modeling techniques and classification based on wavelets networks and neural networks (RBF) for identifying individuals from EMG recordings with 95% accuracy.

There are, additionally, two general ways verification or identification can be managed:

- *one-time*: the user is verified/identified once and remains so indefinitely. Specific conditions can be specified to ensure accurate access with high reliability, before

access to the system is granted. However, since access is never re-verified, there is risk of unauthorised use by someone other than the approved user.
- *on-going*: verification/identification is periodically repeated. This removes the potential for unauthorised use, but potentially reduces verification accuracy as a result of requiring frequently repeating verification exercises.

The works discussed above show that one-time biometric verification and identification is possible via a range of approaches with ECG and EMG signals. But authors are unaware of any biometric verification or identification schemes which provide either on-going re-verification or verification reliant solely on EMG signals of wrist-hand gestures in HCI applications [3]–[5], [8].

B. MOTIVATION

The need for other biometrics to be available critically restricts the capabilities of EMG wearables in secure applications. In these extra hardware for sensing and processing is required to acquire and analyse another bio-physical signal. Within EMG wearables, EMG is acquired from the skin's surface from sensors which are either placed over specific arm muscles (followed by time-frequency EMG analysis), or randomly-placed sensors combined with time-domain analysis [33]. The latter approach brings the considerable advantage that sensors can be placed at any location on the skin, making fitting and use considerably easier. This device is battery-powered and features on-board processing capability, potentially allowing verification or identification on-device, without have to transmit personal EMG recordings to a remote processing resource. In this context, this paper makes the following contributions:
- One-time and on-going biometric verification schemes are presented which consider EMG signals measured at random locations on the skin's surface and provide authentication accuracy exceeding 93%.
- One-time and on-going identification schemes, based on the same EMG acquisition regime, which provide in excess of 92% accurate identification of users.
- Real-time biometric verification and identification using an embedded processor suitable for integration in a portable, battery-powered wearable device.

Section III describes details of developed biometric verification system to enable person authentication based on user EMG signal, with its experimental results after Section IV describes the biometric identification system to recognise person based on their wrist-hand movements EMG signalling, and its performance. Section V details time metrics realisation of developed biometric verification and identification.

III. EMG-BASED BIOMETRIC VERIFICATION

A system employing machine learning is proposed, composed of four main steps *viz*. EMG acquisition and segmentation, feature extraction, projection and classification.

A. EMG ACQUISITION

The EMG acquisition unit houses 8 EMG sensors fitted randomly in circular fashion to a subject's forearm, as shown in Figure 1. Each surface EMG sensor has a sampling frequency of 200 Hz [34], [35]. The armband has a circumference of 19 cm, expandable to 34 cm depending on subject's forearm size. It hosts 8 active surface EMG sensors which can be 0.5–1.8 cm apart. The armband is fitted on the upper forearm so as to cover the maximum hand surface wherein the muscles (also shown in Figure 1) are well sorted [36].

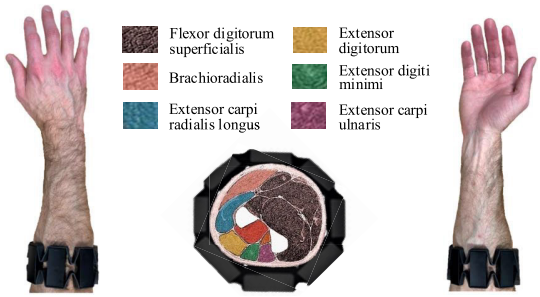

FIGURE 1. Myo Armband placement with cross-section view of upper forearm muscles.

The EMG recording strategy used was similar to the state-of-the-art acquisition and wrist-hand pose classification approach in [7]. The armband was used to record EMG from five subjects (four male and one female) aged between 26 to 34 years. Each was seated on a chair with the shoulder, elbow and forearm are resting on a horizontal surface. The subject then raises their hand perpendicular to the surface and performs one of each of eight movements:

(i) hand open
(ii) wrist flexion
(iii) wrist pronation
(iv) wrist ulnar flexion
(v) wrist supination
(vi) hand close
(vii) wrist extension
(viii) wrist radial flexion

These poses alongside a sample 8-channel EMG recording, are shown in Figure 2. Each pose is held for approximately 10 seconds (a data session), repeated twenty times. The data recording for each of five subject was repeated in each of four consecutive weeks to form an effective multi-session dataset.

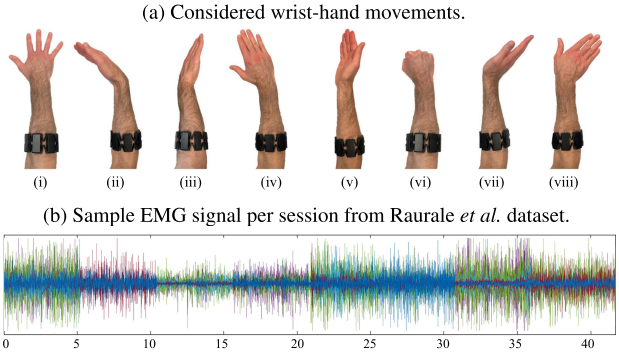

FIGURE 2. Sample EMG signal based on performed wrist-hand movements.

Two other datasets were also considered. The dataset by Raurale *et al.* [37] which includes EMG recordings from ten subjects of 27 ± 4 years is considered. Twenty sessions were recorded from each subject. Each data session consists of continuous EMG recordings of nine movements - hand open, wrist flexion, wrist pronation, wrist ulnar flexion, relaxation, wrist supination, hand close, wrist extension and wrist radial flexion in fixed order. Each movement has approximately five seconds of data recording. The publicly available Angeles *et al.* dataset [38] is also considered, including EMG recordings of fifty healthy subjects (twenty-nine male and twenty-one female) aged between 20 to 59 years performing ten different movements using the same armband. Each performed a movement five times every three seconds in a total of sixteen seconds EMG recording. All performed the same movements - wrist in neutral, pronation, supination, wrist extension, wrist flexion, ulnar deviation, radial deviation, fine pinch, power grip, and hand open - in the same order. These two datasets provide additional sixty users' EMG recording from different sites for building a robust biometric system.

Current wrist-hand EMG analysis techniques employ processing on 256 sample windows of data per sensor, with successive windows offset from one another by 128 ms [7]. We use the same, imposing the requirement that if real-time authentication is to be realised, it must execute in less than 128 ms on the on-board ARM processor [7].

An authentication approach is proposed based on a user by performing at least one of the approved movements. The approach uses features extracted from the EMG signals acquired from the armband followed by dimensionality reduction and classification.

B. FEATURE EXTRACTION

The external appearances of two peoples' gestures might look identical, but the characteristic EMG signals are different due to involved muscle strength. Placed-sensor EMG acquisition approaches, which measure EMG signals from the skin's surface directly over specific arm muscles, allow for effective frequency-domain EMG analysis due to the unique frequency composition of each muscle's EMG [39]. Since the acquisition approach used here is, however, based on randomly-located sensors, frequency-domain specialisation is ineffective. Hence time-domain analysis is used [2], [33], [35]. We propose to use two such features to differentiate users from one another:

- **Band Power** (BP) estimates the average power applied by the user in an EMG signals. It varies according to muscle strength within various movements [40], measuring the average absolute square value of the EMG signal amplitude in a segment [41]:

$$BP = \frac{1}{N}\sum_{n=1}^{N} |x\,[n]\,|^2 \tag{1}$$

where $x\,[n]$ represents n^{th} sample in an EMG signal and N denotes length of the segmented EMG window.

- **Root absolute Sum Square** (RSS) estimates non-fatigue in muscle contraction levels during movement [2], [40]:

$$RSS_{\mathbf{v}} = \sqrt{\sum_{n=1}^{N} |x\,[n]\,|^2} \tag{2}$$

Given an EMG signal segment $X_N \in \mathbb{R}^{N\times 8}$ - where in this case $N = 256$ - each feature is derived from each window acquired from each sensor to result in a feature vector $\mathbf{f}_c \in \mathbb{R}^8$, with the composite of the two vectors $\mathbf{f}_{\mathrm{v}} \in \mathbb{R}^{16}$ derived by concatenation. The resulting feature vector $\mathbf{f}_{\mathrm{v}}$ is considered as a unique biometric feature type to differentiate subject's identity. The variation in the normalised amplitude for these features, across each channel for each wrist-hand movement is summarised in Figure 3.

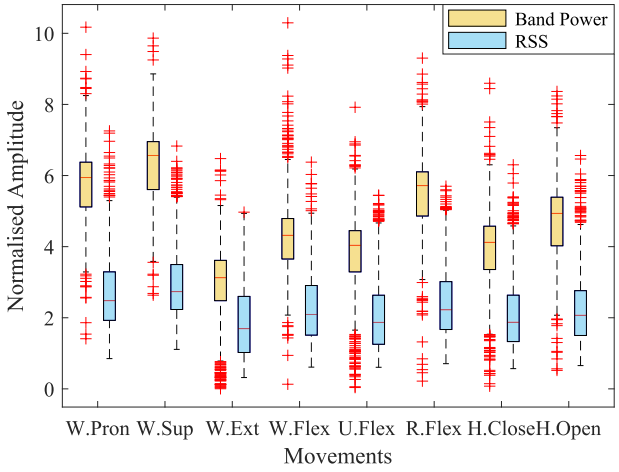

FIGURE 3. Feature amplitude variation based on different wrist-hand movements.

C. FEATURE PROJECTION AND CLASSIFICATION

Feature projection reduces the dimensionality of the feature vectors by projection onto a lower-dimensional space via a mapping function [40]. Linear mapping is optimum for two-class separation [42], which holds for our system since each user is classified as either authenticated or not authenticated. Thus, linear models are generally preferred due to higher reliability in discriminating unseen cases in binary class separation [43]. The projected features are subsequently classified using a feature classification approach. Using area under the operating characteristic curve (AUC) to measure the degree of separability to which the model is capable of distinguishing between classes, AUC metrics for different classifiers with respect to different linear projection schemes are given in Table 1.

The LDA projection based Multi-layer Perceptron (MLP) and the Radial Basis Function (RBF) neural network classifier shows higher AUC values. The LDA projection with MLP is chosen over RBF neural network based on lower complexity within our proposed system. The number of hidden layers ($n = 3$) within MLP was selected based on the

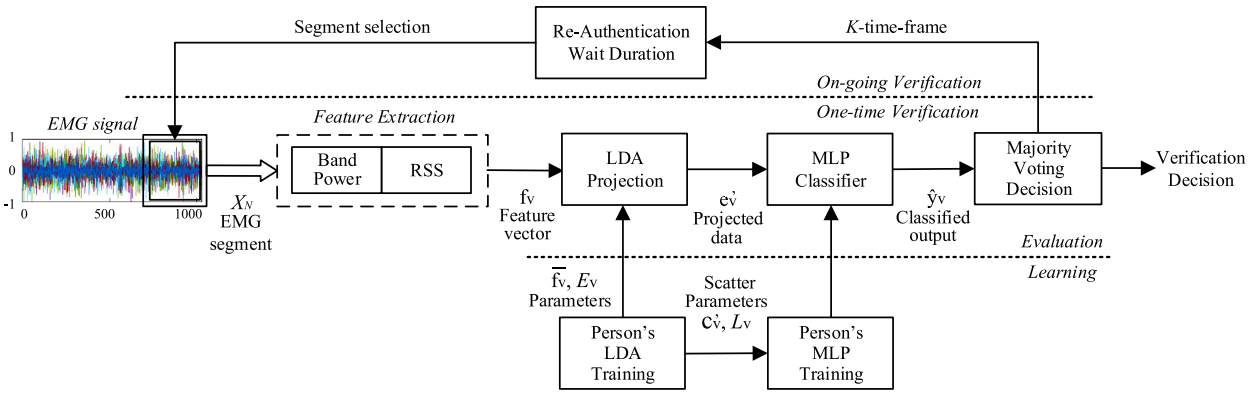

FIGURE 4. Proposed EMG biometric verification system.

TABLE 1. Biometric verification system performance based on different projection and classification techniques.

	Decision trees	MLP	Polynomial-SVM*	RBF-NN**
PCA	0.9079	0.9135	0.9117	0.9131
ICA	0.8948	0.9028	0.9042	0.9029
LDA	0.9087	0.9162	0.9138	0.9167

*For SVM, the polynomial kernel was linear. **For RBF-NN, the parameters was selected based on k=5-fold cross-validation

empirical observation of the error rate as the number of layers was varied. For a range of 10 to 30 neurons, the twenty-two neurons configuration was selected based on optimum verification performance evaluated from k-fold cross-validation ($k = 5$). The output layer has two neurons, one each to indicate authenticated/not authenticated. The resulting system configuration is illustrated in Figure 4.

D. SYSTEM CONFIGURATION

To train the system, a subset (approximately 50%) of each of the three datasets are used

- *Extracted*: the first week's recordings (20 sessions with 160 windows per movement) is used for training
- *Raurale*: 10 sessions (30 windows per movement)
- *Angeles*: 3 sessions (14 windows per movement)

Each window is 256 samples and from each is derived $\mathbf{f}_v \in \mathbb{R}^{h_v}$. These vectors are derived from each channel - where a channel corresponds to the data emanating from a single EMG sensor - separately. Thus, for subject enrollment, 20 sessions of recorded data produces a total of $\mathbf{j}_v = 25600$ feature vectors per subject; 10 sessions from the Raurale dataset produces $\mathbf{j}_v = 2400$ feature vectors per subject and 3 sessions from the Angeles dataset produces $\mathbf{j}_v = 336$ feature vectors per subject. Similarly, $\mathbf{j}_v'$-feature vectors are evaluated in same proportion as false subject class. Hence the training data set for each subject is derived as $D_v \in \mathbb{R}^{(\mathbf{j}_v+\mathbf{j}_v')\times h_v}$; a class label vector $c_v \in \mathbb{R}^{(\mathbf{j}_v+\mathbf{j}_v')}$ for each subject is included for the purposes of training.

Training the LDA derives the following parameters:

1) Mean feature-vector $\bar{\mathbf{f}}_v \in \mathbb{R}^{h_v}$ of D_v;
2) Matrix of eigenvectors $E_v \in \mathbb{R}^{p_v \times h_v}$ where $p_v = 8$ of D_v;
3) Scatter feature projection matrix $L_v \in \mathbb{R}^{\mathbf{j}_v \times p_v}$ of D_v;
4) Vector of class labels $\mathbf{c}_v' \in \mathbb{R}^{\mathbf{j}_v}$ representing D_v;
5) Vector $\mathbf{e}_v \in \mathbb{R}^{p_v}$ of sorted eigenvalues of D_v;

The LDA-derived scatter matrix L_v is also used to train the MLP. The MLP weights and bias are initially drawn from a uniform distribution with a mean and variance of 0 and 1, respectively. The learning process terminates when the absolute rate of change in the average squared error (θ) per iteration was sufficiently small ($\theta \leq 0.1$) [44].

E. EVALUATION - ONE-TIME VERIFICATION

The trained model is tested from the remaining unseen data from each of the three datasets. Algorithm 1 outline the process of one-time verification of a user based on their EMG $X_N \in \mathbb{R}^{N\times c}$. This is interpreted as a set of $N = 256$ sample windows from each of the $c = 8$ EMG channels. These are combined with eigenvectors E_v and mean feature vector $\bar{\mathbf{f}}_v$ into an output vector $\widehat{\mathbf{y}}_v$ indicating verification or otherwise.

Algorithm 1 EMG Verification Algorithm

Input: $X_N, \bar{\mathbf{f}}_v, E_v$
Output: $\widehat{\mathbf{y}}_v$

$c \leftarrow 1 : 8$;
for each $\mathbf{x}_c \in \mathbb{R}^N$ **do**
  $as = \sum_{n=1}^{N} |x(n)|$;
  $BP = as^2/N$;
  $RSS = \sqrt{BP}$;
  $\mathbf{f}_c = [BP, RSS]$;
end for
Compute feature vector $\mathbf{f}_v = [\mathbf{f}_1, \mathbf{f}_2, \mathbf{f}_3, \cdots \mathbf{f}_c]$;
Compute deviation in feature vector $\mathbf{f}_v' = \mathbf{f}_v - \bar{\mathbf{f}}_v$;
Analyse project class vector $\mathbf{e}_v' = \mathbf{f}_v' \times E_v^T$
Evaluate $\widehat{\mathbf{y}}_v$ from trained MLP parameters from $\mathbf{e}_v'$;

Initially an EMG window is extracted from each of the $c = 8$ channels $\mathbf{x}_c \in \mathbb{R}^{256}$ (line 2) and the features are evaluated. The sum of absolute value *as* (line 3) is derived from $\mathbf{x}_c$ to extract *BP* feature (line 4) and root mean square *RSS* feature (line 5). The resulting feature vectors $\mathbf{f}_c \in \mathbb{R}^2$ (line 6) from each of $c = 8$ channels are concatenated into $\mathbf{f}_v \in \mathbb{R}^{16}$ (line 8). The deviation in feature vector $\mathbf{f}'_v$ (line 9) is evaluated to derive projected class vector $\mathbf{e}'_v \in \mathbb{R}^{p_v}$ is derived from $\overline{\mathbf{f}_v}$ and E_v (line 10). The result $\widehat{\mathbf{y}}_v \in \mathbb{R}^2$ is evaluated from the trained model parameters from $\mathbf{e}'_v$ (line 11).

Since verification occurs only once, a single wrist-hand pose - that with the highest verification accuracy - can be used; users hold that pose for a short period of time whilst being identified. The major questions concern the selection of pose and the duration for which it should be held.

Average verification accuracy across three different datasets for each pose based on the feature set $\mathbf{f}_v$ with LDA projection and different feature classification techniques are detailed in Table 2. The hyper parameters for classifiers are selected from 5-fold cross-validation techniques in the training dataset. The average classification accuracy for MLP and RBF-NN classifiers shows higher performance compared to decision tree and polynomial-SVM classifiers. The MLP classifier before LDA projection is chosen within our system pipeline based on lower complexity. When considered window-by-window, wrist pronation is the least reliable movement, with an average accuracy of 84.40% across all three dataset. Hand close and wrist extension poses show most verification promise, with average accuracies of 95.71% and 93.41% respectively. Considering all eight wrist-hand poses provide an average accuracy of 91.66% is achieved.

TABLE 2. Verification accuracy with LDA and different classifier across different movements.

	Verification Accuracy (%)			
Movements	**Decision trees**	**MLP**	**SVM**	**RBF-NN**
Hand Open	94.46	92.82	90.97	92.29
Hand Close	89.35	95.71	94.15	96.28
Wrist Flexion	91.48	90.79	92.42	90.28
Wrist Extension	88.28	93.41	92.39	93.92
Wrist Pronation	87.69	84.40	85.89	84.19
Wrist Supination	89.63	90.96	91.58	91.26
Wrist Ulnar Flexion	91.05	93.23	92.11	93.36
Wrist Radial Flexion	90.26	91.98	91.53	92.05
Average	**90.28**	**91.66**	**91.38**	**91.70**

To reduce the number of errors, majority-voting, i.e. verification based on the results of multiple EMG windows, is considered. Specifically, 5-majority configurations are considered, making decisions on the basis of five windows respectively. The results, shown in Table 3 show improved accuracy across all datasets, with accuracy of more than 99% for the Raurale dataset. The limited number of training data samples and larger number of subjects in the Angeles dataset, results in lower verification performance. Thus, the average verification accuracy exceeds 92% for one-time authentication. Authentication in these cases is near-instant, requiring only a single window. In the case where a short time period (up to five windows, or approximately 2 s) can be considered, hand-close and wrist extension can also be considered.

TABLE 3. One-time verification with majority voting.

Dataset	**Accuracy**	**Precision**	**Recall**	**F1-score**
Multi-session	97.34	96.57	98.18	97.37
Raurale *et al.*	99.08	98.84	99.31	99.09
Angeles *et al.*	81.19	79.78	85.56	81.63
Average (%)	**92.54**	**91.73**	**94.35**	**92.70**

The genuine and imposter score vectors are used to produce the Receiver Operating Characteristic (ROC) curve which shows the rate of false acceptance against the false rejection. The ROC curves for each dataset are shown in Figure 5.

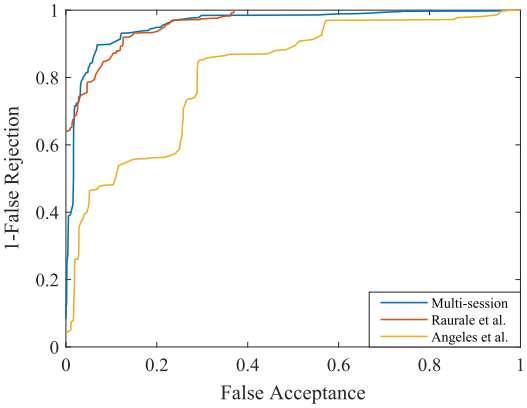

FIGURE 5. Per-dataset ROC for Biometric Verification System.

F. EVALUATION - ON-GOING VERIFICATION

On-going verification repeats periodically; we analyse the performance of this approach based on re-verification intervals of 1024 samples (approximately 5 seconds), 2048 samples (approximately 10 seconds) and 3072 samples (approximately 15 seconds). Since it is not feasible to insist that the user repeat the same wrist-hand pose with these frequencies, on-going verification required *all* movements to be considered. Under this condition and verification based on a single window, the ongoing re-verification accuracy across all sixty-five users performing eight wrist-hand movements in majority voting configuration is illustrated in Figure 6.

As this describes, the average accuracy varies between 79% to 98% for a 1024 sample interval across different dataset. With a 3072-sample interval, the average accuracy of over 93% is observed from all three dataset.

The Equal Error Rate (EER) is used to measure accuracy by gauging the point where False Acceptance Rate (FAR) and

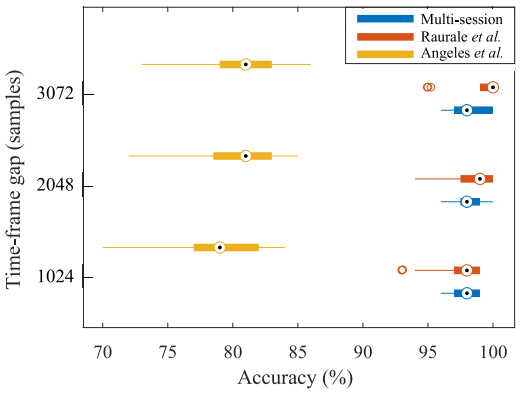

FIGURE 6. On-going verification accuracy across all users in different dataset based on different time-frame interval. The dots represent average values, thick lines represents the inter-quartile range, and thin lines represent the accuracy over all subjects.

False Rejection Rate (FRR) equal one-another. This is shown, for all users for both one-time and on-going verification in Figure 7.

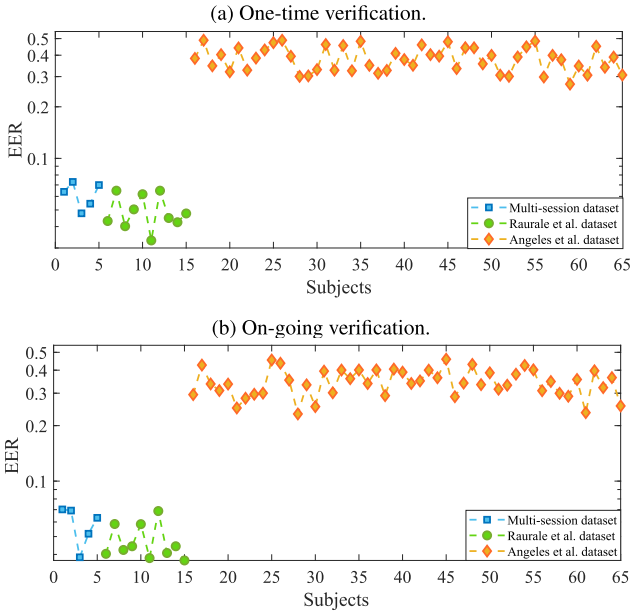

FIGURE 7. Biometric verification performance in different system modes.

Further, the average verification performance across each of three dataset is analysed for both modes as quoted in Table 4. The performance parameters are compared with the existing state-of-the-art in EMG and ECG biometric verification system in order to justify the proposed system's capability.

The average EER value from all three datasets for one-time and on-going verification system evaluated as 16.34% and 15.98%. The proposed verification system in both modes provides higher accuracy than the Belgacem *et al.* [21] EMG verification approach. The state-of-the-art ECG based verification approaches [19], [20] show superior performance to

TABLE 4. Biometric verification performance comparison.

Systems		Subjects	Accuracy (%)	EER (%)
Proposed System	One-time	65	92.54	16.34
	On-going		93.26	15.98
Hammad *et al.* [19]		455	98.94	3.65
Hammad *et al.* [20]		390	99.06	1.04
Belgacem *et al.* [21]		60	90.00	–

the proposed EMG-based system. This is to be expected - an ECG signal usually has a more consistent and stable behaviour than the highly dynamic EMG which varies in form significantly between users, the wide range of movements permissible by this approach. However, this approach is focused on systems where EMG is the *sole* signal via which users can be authenticated and it is the first to demonstrate effective performance in this regard.

IV. EMG BIOMETRIC IDENTIFICATION SYSTEM

Authentication does not individually identifying users, but in many cases this may be required. This section analyses the use of EMG signals in this identification process.

A. AMPLITUDE NORMALISATION AND FEATURE EXTRACTION

Every person has their own unique muscle strength, manifest as varying EMG amplitudes for different wrist-hand movements [2], [33]. Different muscles show different amplitude levels during different movements [33], [34]. Amplitude normalisation forms an average amplitude for each person based on their varying EMG amplitude signalling range. The average amplitude expresses the power involved at that instant [40]. Mean normalisation is used to normalise the average of segmented EMG signal [45] and is expressed as,

$$\mathbf{s}_N = \frac{x[n]}{\frac{1}{N}\sum_{n=1}^{N}|x[n]|} \tag{3}$$

Further, the feature is extracted from the normalised signal in order to derive a unique value for each person. Root sum square (RSS) is used to represent the muscle contraction level during movement [2], [46], giving a different scaling for every person. It is expressed as [46],

$$s_{RSS} = \sqrt{\sum_{n=1}^{N}|s\,[n]\,|^2} \tag{4}$$

where $s[n]$ represents the normalised signal. The s_{RSS} coefficient evaluated from each channel are concatenated to form a feature vector vector $\mathbf{f}_i \in \mathbb{R}^8$. The value for each feature coefficient is evaluated from EMG signals for each person as the mean feature value from eight wrist-hand movements. The feature vectors combine via projection and classification to help distinguish different subjects more precisely.

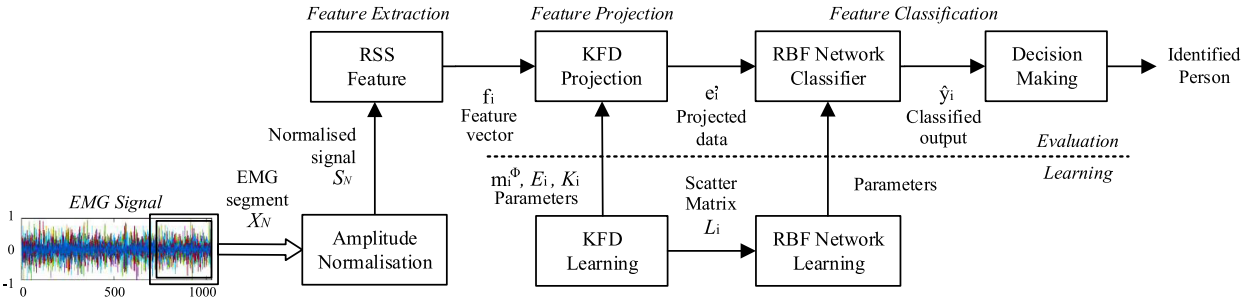

FIGURE 8. Proposed EMG Biometric Identification system.

B. FEATURE PROJECTION AND CLASSIFICATION

Linear mapping leads to poorer between-class separation in multi-class analysis [47] and non-linear model structures consisting of arbitrarily shaped clusters manifolds leads to better multi-class analysis, and is preferred to avoid class overlapping [48]. The non-linear polynomial Kernel Principal Component Analysis (KPCA) [49] and Kernel Fisher Discrimination (KFD) analysis [50] have been successively used for projecting multi-class features. Both non-linear projection schemes are considered and are combined with different feature classifiers. The average AUC metrics of projection techniques with respect of different feature classification approaches as shown in Table 5.

TABLE 5. Biometric identification system performance based on different projection and classification techniques.

	Decision trees	MLP†	Gaussian-SVM††	RBF-NN
KPCA	0.9126	0.9205	0.9116	0.9228
KFD	0.9161	0.9197	0.9183	0.9246

†For MLP, same configuration is used as of Section III-C. ††For SVM, the gaussian kernel was RBF and hyper parameters were selected based on k=5-fold cross-validation.

The RBF neural network with KFD projection analysis shows highest AUC and thus are selected for the system pipeline. The RBF neural network is configured with two hidden layers of ten and eight RBF nodes, selected based on the lowest learning error analysed as the number of layers and nodes combination was varied within k-fold cross-validation (where $k = 5$) approach. Weights and bias were initialised before training from a uniform distribution with a mean and variance of 0 and 1, respectively. The learning process was stopped when the absolute rate of change in the average squared error per iteration was sufficiently small ($\theta \leq 0.1$) [44]. The output layer has sixty-five nodes corresponding to each validated person. While in system evaluation phase, the maximum output of the RBF node in the output layer was selected as the identified person for the provided KFD feature subspace. Thus, the overall proposed EMG biometric identification system architecture is summarised in Figure 8.

C. SYSTEM EVALUATION

During training, each 256-sample window is amplitude normalised and an RSS feature vector $\mathbf{f}_i \in \mathbb{R}^c$ ($c = 8$ as per (4)) derived from the amplitude normalised signal $\mathbf{s}_N$. For training, three data sources are again used - the first week's 20 recorded sessions (1280 windows per session from eight movements) is combined with 10 sessions (240 windows per session) in the Raurale datset and 3 sessions (112 windows per session) in the Angeles datset. Thus, a total of 25600 feature vectors per subject are retrieved from the multi-session dataset, 2400 per subject from Raurale dataset and 336 feature vectors per subject from Angeles dataset. This results in a training data frame $D_i \in \mathbb{R}^{j_i \times c}$ where, $j_i = 168800$, followed by the corresponding column class label frame defining each feature data class in D_i. This is used to train the KFD model for derivation of:

1) Mean feature-vector $\mathbf{m}_i^{\Phi} \in \mathbb{R}^c$ of D_i;
2) Matrix of eigenvectors $E_i \in \mathbb{R}^{p_i \times c}$ ($p_i = 8$) of D_i;
3) Matrix of kernel feature coefficients $K_i \in \mathbb{R}^{p_i \times c}$ of D_i;
4) Matrix of scatter feature projection $L_i \in \mathbb{R}^{J_i \times p_i}$ of D_i;
5) Vector of class labels $\mathbf{c}_i' \in \mathbb{R}^{\mathbf{j_i}}$ representing D_i;
6) Vector $\mathrm{e}_i \in \mathbb{R}^{p_i}$ of sorted eigenvalues of D_i;

While training the RBF neural network, the derived scatter matrix L_i from KFD analysis is used with that of weights and bias RBF analysis in the graph.

During evaluation, accuracy is tested on trained RBF network parameters with the remaining session data by evaluating a feature vector and its projected class vector from KFD analysis parameters. Algorithm 2 shows the steps in translating the segmented input signal $X_N \in \mathbb{R}^{N \times c}$ ($N = 256$ window for each of the $c = 8$ EMG channels), E_i and $\bar{\mathbf{f}}_i$ into an output vector $\widehat{\mathbf{y}}_i \in \mathbb{R}^i$ indicating $i = 65$ person's identity.

The EMG segment is extracted from each of the $c = 8$ channels $\mathbf{x}_c \in \mathbb{R}^{256}$ (line 2) with the mean μ derived from $\mathbf{x}_c$ (line 3). The normalised vector $\mathrm{s}_N \in \mathbb{R}^N$ from μ and $\mathbf{x}_c$ for the N^{th} iteration is derived in line 5. The absolute sum value ss is derived from the normalised matrix s_N in line 7, and the RSS-feature vector $\mathrm{f}_i \in \mathbb{R}^c$ from ss in line 8. The deviation of feature vector $\mathbf{f}_i' \in \mathbb{R}^c$ is calculated from $\mathbf{f}_i$ and $\mathbf{m}_i^{\Phi}$ (line 10), followed by projection class vector $\mathbf{e}_i' \in \mathbb{R}^{p_i}$ (line 11). Finally, the output $\widehat{\mathbf{y}}_i$ is evaluated from $\mathbf{e}_i'$ (line 12).

Algorithm 2 EMG Identification Algorithm

Input: X_N, $\mathbf{m}_i^{\Phi}$, E_i, K_i
Output: $\widehat{\mathbf{y}}_i$

$c \leftarrow 1:8$;
for each $\mathbf{x}_c \in \mathbb{R}^N$ **do**
  $\mu = \sum_{n=1}^{N} x(n) / N$;
  for $n = 1$ to N **do**
    $\mathbf{s}_n = x(n)/\mu$;
  end for
  $ss = \sum_{n=1}^{N} |s(n)|$;
  $\mathbf{f}_i(c) = \sqrt{ss^2/N}$;
end for
Compute deviation in feature vector $\mathbf{f}'_i = \mathbf{f}_i - \mathbf{m}_i^{\Phi}$;
Analyse project class vector $\mathbf{e}'_i = \mathbf{f}'_i \times [E_i^T \times K_i]$;
Evaluate $\widehat{\mathbf{y}}_i$ from trained RBF parameters from $\mathbf{e}'_i$;

The remaining 60 sessions from the multi-session dataset, 10 sessions from Raurale dataset and 3 sessions from Angeles dataset are tested. Identification performance for single-window with 5-majority voting on the feature set $\mathbf{f}_i$ with selected KFD-RBF classification parameters from 5-fold cross-validation techniques are itemised in Table 6.

TABLE 6. One-time identification performance for different system configurations.

Configuration	Accuracy	Precision	Recall	F1-score
Single-window	90.58	63.26	90.35	74.42
Majority voting	91.28	65.18	91.25	76.05

With 5-majority voting, identification accuracy improved by 0.7% compared to single-window. False identification was observed in around 8% of cases. With the set majority voting configuration, the identification performance per movement is evaluated as illustrated in Figure 9. Identification via wrist extension and hand close movements shows more than 95% accuracy, with wrist pronation the poorest at 87.77%. For optimum one-time biometric person identification, the hand close and wrist extension could be preferred choice.

D. EVALUATION - ON-GOING IDENTIFICATION

On-going identification performance is analysed for re-identification intervals of 1024 samples, 2048 samples and 3072 samples. Based on this configuration, the ongoing re-identification accuracy across all ten users performing nine wrist-hand movements are described in Table 7.

The re-identification accuracy varies between 90% for a 1024 sample interval and with 2048, 3072-sample interval gap, the re-identification accuracy is above 91%. The maximum re-identification accuracy of 92.08% is achieved with 3072-sample interval in 5-majority voting configuration, thus, considered optimal as regards identification accuracy.

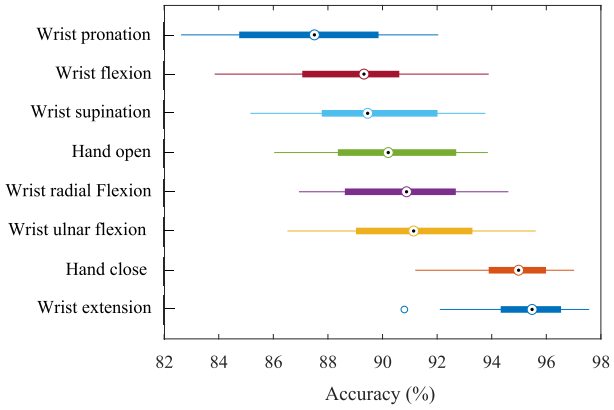

FIGURE 9. Identification accuracy across different movements. The dots represent average values, thick lines represents the inter-quartile range, and thin lines represent the accuracy over all subjects.

TABLE 7. On-going identification accuracy for different system configurations.

System Configuration	Time-frame gap (K) 1024	2048	3072
Single-window	90.92	91.54	91.67
Majority voting	91.39	91.92	92.08

The EER for the different system modes are compared with the state-of-the-art EMG identification systems, as itemised in Table 8. It is observed that the proposed system in both modes provides the identification accuracy of over 91% with EER value of around 17%. This is not only highly desirable for biometric identification in practice but also the one of highest when compared with leading EMG-based biometric identification approaches according to number of subjects considered [22]–[24].

TABLE 8. Biometric identification performance comparison values.

Systems		Subjects	Accuracy (%)	EER (%)
Proposed system	One-time	65	91.28	17.28
	On-going		92.08	16.42
Kim *et al.* [22]		28	86.66	–
Suresh *et al.* [23]		49	73.33	–
Chantaf *et al.* [24]		10	95.00	–

V. SYSTEM IMPLEMENTATION

This section considers whether the proposed biometric verification and identification approaches can be realised in real-time within the computation power of EMG wearables such as that used for acquisition in this paper.

For real-time behaviour, processing time should be less than the window increment, which is 128 ms in our case.

To influence real-time computation on a battery-operated embedded processor, the biometric systems are deployed on a 1.4 GHz ARM Cortex-A53 Raspberry Pi 3 B+ platform. The biometric authentication systems C++ code is deployed in the Raspberry Pi 3 B+ platform build with Broadcom 64-bit ARM Cortex-A53 Processor. The processing times of each operation are quoted in Table 9.

TABLE 9. ARM Cortex A-53 processing time metrics for Biometric systems.

(a) Biometric verification system

Operations	time (ms)
BP	0.24
RSS_v	0.16
LDA	0.21
MLP	0.38
Others	0.07
Total	**1.06**

(b) Biometric identification system

Operations	time (ms)
Normalisation	0.41
RSS_i	0.23
KFD	0.36
RBF	0.52
Others	0.09
Total	**1.61**

As illustrated in Table 9, the proposed biometric verification approach executes in 1.06 ms and 1.61 ms for identification on the ARM Cortex-A53 which is again 120 and 79 times lower enough to process each 128 ms EMG window interval in real-time. Further, when combined with the wrist-hand pose identification system from [37]. The wrist-hand pose identification system [37] with similar system configuration, shows executing an EMG segment in 9.75 ms on the ARM Cortex-A53. Thus, the combined verification/identification and pose identification system would execute in 10.81/11.36 ms - well inside the 128 ms EMG window for real-time computation.

VI. CONCLUSION

This paper proposes a first-in-kind biometric system which uses forearm EMG acquired as a result of wrist-hand movement to enable accurate verification and identification using time-domain pattern recognition. It acquires EMG from randomly-placed sensors. It employs time-domain features followed by a combination of LDA-based projection of the resulting feature vector and MLP classification of the resulting data into true or false categories. The one-time verification system show over 92% accuracy with 27.79% EER evaluated across all considered wrist-hand movements with 5-majority voting. Further, the progressive on-going verification system performance shows up to 93% re-verification accuracy for 15.36 s time-frame interval, removing the prospect for unauthorised use.

When used for identification, 256-sample EMG segments are amplitude normalized and form a time-domain feature which is projected using KFD and classified by RBF-NN. Identification was 91% accurate with 17.28% EER in one time-verification and 92% accurate with 16.42% EER in progressive on-going identification for all eight wrist-hand movements. When deployed on ARM Cortex A-53 embedded processor representative of the kind used in EMG wearable such as that used for acquisition in this paper, the proposed authentication system requires 1.06 ms to execute per 256-sample EMG window, with the identification system requiring 1.61 ms. Both systems add negligible overhead where both wrist-hand movement detection and verification or identification need to be performed in a single window; the total run-time is still well inside the 128 ms target. Thus, the proposed EMG biometric systems shows advantage for real-time realisation on battery-operated hardware platforms without repeating the same wrist-hand pose.

REFERENCES

[1] A. Schmidt, "Biosignals in human-computer interaction," *Interactions*, vol. 23, no. 1, pp. 76–79, Dec. 2015.

[2] S. Kakei, "Muscle and movement representations in the primary motor cortex," *Science*, vol. 285, no. 5436, pp. 2136–2139, Sep. 1999.

[3] Manus-VR. *Wearable Manus Gloves*. Accessed: Nov. 10, 2020. [Online]. Available: https://manus-vr.com/mocap-gloves

[4] Biometrics-ltd. *DataLite Device*. Accessed: Nov. 10, 2020. [Online]. Available: https://www.biometricsltd.com/datalite

[5] Ottobock-ltd. *Bebionic Upper Limbs Prosthetic Hand*. Accessed: Nov. 10, 2020. [Online]. Available: https://www.ottobockus.com/prosthetics/upper-limb-prosthetics/solution-overview/bebionic-hand

[6] R. Merletti and P. A. Parker, *Electromyography: Physiology, Engineering, and Non-Invasive Applications*, vol. 11. Hoboken, NJ, USA: Wiley, 2004.

[7] J.-U. Chu, I. Moon, Y.-J. Lee, S.-K. Kim, and M.-S. Mun, "A supervised feature-projection-based real-time EMG pattern recognition for multifunction myoelectric hand control," *IEEE/ASME Trans. Mechatronics*, vol. 12, no. 3, pp. 282–290, Jun. 2007.

[8] E. Mattar, "A survey of bio-inspired robotics hands implementation: New directions in dexterous manipulation," *Robot. Auto. Syst.*, vol. 61, no. 5, pp. 517–544, May 2013.

[9] M. Karnan, M. Akila, and N. Krishnaraj, "Biometric personal authentication using keystroke dynamics: A review," *Appl. Soft Comput.*, vol. 11, no. 2, pp. 1565–1573, Mar. 2011.

[10] S. P. Banerjee and D. Woodard, "Biometric authentication and identification using keystroke dynamics: A survey," *J. Pattern Recognit. Res.*, vol. 7, no. 1, pp. 116–139, 2012.

[11] J. Zhao, Z. Xie, L. Jiang, H. Cai, H. Liu, and G. Hirzinger, "EMG control for a five-fingered underactuated prosthetic hand based on wavelet transform and sample entropy," in *Proc. IEEE/RSJ Int. Conf. Intell. Robot. Syst.*, Oct. 2006, pp. 3215–3220.

[12] K. Revett, F. Deravi, and K. Sirlantzis, "Biosignals for user authentication–towards cognitive biometrics?" in *Proc. Int. Conf. Emerg. Secur. Technol.*, Sep. 2010, pp. 71–76.

[13] U. Uludag, A. Ross, and A. Jain, "Biometric template selection and update: A case study in fingerprints," *Pattern Recognit.*, vol. 37, no. 7, pp. 1533–1542, Jul. 2004.

[14] M. El-Abed, R. Giot, B. Hemery, and C. Rosenberger, "A study of users' acceptance and satisfaction of biometric systems," in *Proc. 44th Annu. IEEE Int. Carnahan Conf. Secur. Technol.*, Oct. 2010, pp. 170–178.

[15] J. Rigelsford, "Biometric authentication," *Sensor Rev.*, vol. 23, no. 4, pp. 13–28, Dec. 2003.

[16] J. Daugman, "New methods in iris recognition," *IEEE Trans. Syst., Man, Cybern. B. Cybern.*, vol. 37, no. 5, pp. 1167–1175, Oct. 2007.

[17] A. K. Jain, A. Ross, and S. Prabhakar, "An introduction to biometric recognition," *IEEE Trans. Circuits Syst. Video Technol.*, vol. 14, no. 1, pp. 4–20, Jan. 2004.

[18] M. Ingale, R. Cordeiro, S. Thentu, Y. Park, and N. Karimian, "Ecg biometric authentication: A comparative analysis," *IEEE Access*, vol. 8, pp. 117853–117866, 2020.

[19] M. Hammad, S. Zhang, and K. Wang, "A novel two-dimensional ECG feature extraction and classification algorithm based on convolution neural network for human authentication," *Future Gener. Comput. Syst.*, vol. 101, pp. 180–196, Dec. 2019.

[20] M. Hammad, P. Páawiak, K. Wang, and U. R. Acharya, "ResNet-attention model for human authentication using ECG signals," *Expert Syst.*, vol. 4, p. e12547, Mar. 2020.

[21] N. Belgacem, R. Fournier, A. Nait-Ali, and F. Bereksi-Reguig, "A novel biometric authentication approach using ECG and EMG signals," *J. Med. Eng. Technol.*, vol. 39, no. 4, pp. 226–238, May 2015.
[22] J. S. Kim and S. B. Pan, "A study on EMG-based biometrics," *J. Internet Services Inf. Secur.*, vol. 7, no. 2, pp. 19–31, May 2017.
[23] M. Suresh, P. G. Krishnamohan, and M. S. Holi, "GMM modeling of person information from EMG signals," in *Proc. IEEE Recent Adv. Intell. Comput. Syst.*, Sep. 2011, pp. 712–717.
[24] S. Chantaf, L. Makni, and A. Nait-Ali, "Single channel surface EMG based biometrics," in *Hidden Biometrics*. Singapore: Springer, 2020, pp. 71–90.
[25] V. I. Ivanov and J. S. Baras, "Authentication of swipe fingerprint scanners," *IEEE Trans. Inf. Forensics Security*, vol. 12, no. 9, pp. 2212–2226, Sep. 2017.
[26] N. Poh, C. H. Chan, J. Kittler, S. Marcel, C. M. Cool, E. A. Ráa, J. L. A. A. Castro, M. Villegas, R. Paredes, V. Štruc, A. A. Salah, H. Fang, and N. Costen, "An evaluation of video-to-video face verification," *IEEE Trans. Inf. Forensics Security*, vol. 5, no. 4, pp. 781–801, Dec. 2010.
[27] A. T. B. Jin, D. N. C. Ling, and A. Goh, "Biohashing: Two factor authentication featuring fingerprint data and tokenised random number," *Pattern Recognit.*, vol. 37, no. 11, pp. 2245–2255, Nov. 2004.
[28] A. Riera, S. Dunne, I. Cester, and G. Ruffini, "STARFAST: A wireless wearable EEG/ECG biometric system based on the ENOBIO sensor," in *Proc. Int. Workshop Wearable Micro Nanosystems Personalised Health*, 2008, pp. 1–4.
[29] I. Brahim, I. Dhibou, L. Makni, S. Said, and A. Nait-Ali, "Wearable multichannel EMG biometrics: Concepts," in *Hidden Biometrics*. Singapore: Springer, 2020, pp. 91–100.
[30] S. Venugopalan, F. Juefei-Xu, B. Cowley, and M. Savvides, "Electromyograph and keystroke dynamics for spoof-resistant biometric authentication," in *Proc. IEEE Conf. Comput. Vis. Pattern Recognit. Workshops (CVPRW)*, Jun. 2015, pp. 109–118.
[31] A. D. C. Chan, M. M. Hamdy, A. Badre, and V. Badee, "Wavelet distance measure for person identification using electrocardiograms," *IEEE Trans. Instrum. Meas.*, vol. 57, no. 2, pp. 248–253, Feb. 2008.
[32] S. A. Israel, W. T. Scruggs, W. J. Worek, and J. M. Irvine, "Fusing face and ECG for personal identification," in *Proc. 32nd Appl. Imag. Pattern Recognit. Workshop*, Oct. 2003, pp. 226–231.
[33] C. J. De Luca, "The use of surface electromyography in biomechanics," *J. Appl. Biomechanics*, vol. 13, no. 2, pp. 135–163, May 1997.
[34] S. Greenberg. (2015). *Myo Developer Blog*. Accessed: Feb. 22, 2018. https://developer.thalmic.com/forums/topic/1945/
[35] M. Sathiyanarayanan and S. Rajan, "MYO armband for physiotherapy healthcare: A case study using gesture recognition application," in *Proc. 8th Int. Conf. Commun. Syst. Netw. (COMSNETS)*, Jan. 2016, pp. 1–6.
[36] Delsys. (2016). *Delsys EMG Sensor Placement Technical Note 101*. Accessed: Jul. 9, 2018. [Online]. Available: https://www.delsys.com/downloads/TECHNICALNOTE/101-emg-sensor-placement.pdf
[37] S. A. Raurale, J. McAllister, and J. M. del Rincon, "Real-time embedded EMG signal analysis for wrist-hand pose identification," *IEEE Trans. Signal Process.*, vol. 68, pp. 2713–2723, Apr. 2020.
[38] I. J. Ramírez Ángeles and M. A. Aceves Fernández. (2018). *Multichannel Electromyography Signal Acquisition of Forearm*. [Online]. Available: https://data.mendeley.com/datasets/p77jn92bzg/1, doi: 10.17632/p77jn92bzg.1.
[39] A. Georgakis, L. K. Stergioulas, and G. Giakas, "Fatigue analysis of the surface EMG signal in isometric constant force contractions using the averaged instantaneous frequency," *IEEE Trans. Biomed. Eng.*, vol. 50, no. 2, pp. 262–265, Feb. 2003.
[40] A. Phinyomark, P. Phukpattaranont, and C. Limsakul, "Feature reduction and selection for EMG signal classification," *Expert Syst. Appl.*, vol. 39, no. 8, pp. 7420–7431, Jun. 2012.
[41] W. Klimesch, H. Schimke, and J. Schwaiger, "Episodic and semantic memory: An analysis in the EEG theta and alpha band," *Electroencephalogr. Clin. Neurophysiol.*, vol. 91, no. 6, pp. 428–441, Dec. 1994.
[42] C. Chatterjee and V. P. Roychowdhury, "On self-organizing algorithms and networks for class-separability features," *IEEE Trans. Neural Netw.*, vol. 8, no. 3, pp. 663–678, May 1997.
[43] D. J. Hand, "Discrimination and classification," *Wiley Series in Probability and Mathematical Statistics*. Hoboken, NJ, USA: Wiley, 1981.
[44] S. Haykin, *Neural Networks: A Comprehensive Foundation*. Upper Saddle River, NJ, USA: Prentice-Hall, 1994.
[45] A. M. Burden, M. Trew, and V. Baltzopoulos, "Normalisation of gait EMGs: A re-examination," *J. Electromyogr. Kinesiol.*, vol. 13, no. 6, pp. 519–532, Dec. 2003.
[46] R. J. Moffat, "Describing the uncertainties in experimental results," *Experim. Thermal Fluid Sci.*, vol. 1, no. 1, pp. 3–17, Jan. 1988.
[47] V. Roth and V. Steinhage, "Nonlinear discriminant analysis using kernel functions," in *Proc. Adv. Neural Inf. Process. Syst.*, 2000, pp. 568–574.
[48] S. Mika, G. Ratsch, J. Weston, B. Scholkopf, and K. R. Mullers, "Fisher discriminant analysis with kernels," in *Proc. Neural Netw. Signal Process.*, 1999, pp. 41–48.
[49] K. Xing, P. Yang, J. Huang, Y. Wang, and Q. Zhu, "A real-time EMG pattern recognition method for virtual myoelectric hand control," *Neurocomputing*, vol. 136, pp. 345–355, Jul. 2014.
[50] S. Raurale, J. McAllister, and J. M. del Rincon, "EMG wrist-hand motion recognition system for real-time embedded platform," in *Proc. IEEE Int. Conf. Acoust., Speech Signal Process. (ICASSP)*, May 2019, pp. 1523–1527.

SUMIT A. RAURALE (Member, IEEE) received the B.E. degree in electronics design technology from the Shri Ramdeobaba College of Engineering and Management, Nagpur, India, in 2012, the M.Tech. degree in electronic systems and communication from the Government College of Engineering, Amravati, India, in 2014, and the Ph.D. degree in electrical and electronic engineering from Queen's University of Belfast, U.K., in 2019. He is currently a Postdoctoral Researcher with the Irish Centre for Maternal and Child Health Research (INFANT), University College Cork, Ireland. His research interests include biomedical signal processing, biometrics, human–computer interface, and machine learning.

JOHN MCALLISTER (Senior Member, IEEE) received the Ph.D. degree in electronic engineering from the Queen's University of Belfast, Belfast, U.K., in 2004. He is currently a member of academic staff with the School of Electronics, Electrical Engineering and Computer Science, Queen's University of Belfast. His research interests include resource constrained and embedded signal processing and artificial intelligence. He is the Chair of the IEEE Technical Committee on Design and Implementation of Signal Processing Systems (DISPS), a Senior Area Editor for the IEEE TRANSACTIONS ON SIGNAL PROCESSING, a founding Chief Editor of the IEEE *Signal Processing Society* Resource Center, a co-founder of Analytics Engines Ltd., and a member of the Editorial Board of the *Journal of Signal Processing Systems*.

JESÚS MARTÍNEZ DEL RINCÓN (Member, IEEE) received the B.Sc. degree in telecommunication engineering and the Ph.D. degree in computer vision from the University of Zaragoza, Spain, for his work into the development of tracking algorithms for video surveillance and human motion analysis, in 2003 and 2008, respectively. He is currently a Senior Lecturer with the School of Electronics, Electrical Engineering and Computer Science, Queen's University of Belfast, Belfast, U.K. His main research interest includes deep learning applied to video surveillance and cyber-security.